Desalination and Water Treatment
www.deswater.com

doi: 10.5004/dwt.2023.29843

306 (2023) 236–244
September

Utilization of *Mangifera indica* leaves powder as a cost-effective adsorbent for the removal of eosin yellow from wastewater

Mahreen Iqbal[a], Shagufta Zafar[a], Muhammad Imran Khan[b,*], Shabnam Shahida[c,*], Hafeez ur Rehman[d], Mahwish Iqbal[e], Abdallah Shanableh[b], Tariq Javed[f]

[a]*Department of Chemistry, The Government Sadiq College Women University, Bahawalpur 63000, Pakistan, email: mahreeniqbal08@gmail.com (M. Iqbal), shg_zf@gscwu.edu.pk (S. Zafar)*
[b]*Research Institute of Sciences and Engineering (RISE), University of Sharjah, Sharjah 27272, United Arab Emirates, email: raoimranishaq@gmail.com (M.I. Khan), Shanableh@sharjah.ac.ae (A. Shanableh)*
[c]*Department of Chemistry, University of Poonch, Rawalakot 12350, Azad Kashmir, Pakistan, email: shabnamshahida01@gmail.com*
[d]*The Islamia University of Bahawalpur, Bahawalpur 63100, Pakistan, email: hafeez.rehman@iub.edu.pk*
[e]*Environmental Chemistry Laboratory, Department of Chemistry, University of Agriculture Faisalabad, Pakistan, email: mahwishiqbal2323@gmail.com*
[f]*Department of Chemistry, University of Sahiwal, Sahiwal, Pakistan, email: mtariq@uosahiwal.edu.pk*

Received 6 May 2023; Accepted 12 August 2023

ABSTRACT

The current research was designed to use the *Mangifera indica* (mango) leaves (MIL) powder for eradication of eosin yellow (EY) dye from an aqueous solution at 25°C. Adsorption of eosin yellow (EY) onto MIL powder was investigated by X-ray diffraction. The percentage adsorption of EY was increased with contact time, mass of MIL powder (adsorbent) and temperature while decreased with EY initial concentration. Several non-linear isotherm models were applied in order to investigate EY adsorption onto MIL powder and attained results exhibited that adsorption of EY obeyed non-linear Langmuir isotherm model. Determined maximum theoretical adsorption capacity was 39.67 mg/g. In addition, EY adsorption onto MIL powder was physical adsorption process. Adsorption kinetics of EY adsorption was illustrated by applying non-linear pseudo-first-order and pseudo-second-order models. Attained results exhibited that non-linear pseudo-second-order model fitted to EY adsorption. Thermodynamics investigations represented the endothermic and spontaneous nature of EY adsorption process. The desorption of EY from MIL powder was also studied.

Keywords: *Mangifera indica* leaves powder; Dye wastewater treatment; Adsorption; Eosin yellow; Acid-treated biomass; Pseudo-second-order model; Endothermic process; Langmuir isotherm

1. Introduction

In particular, synthetic dyes were used for leather and textile dyeing, additives for petroleum products, paper printing and color photography [1]. Among most commonly used dyes, reactive dyes are gaining importance because of high color fastness, vivid colors and luxury usages [2,3]. They displayed different chemical structures. It was caused by substituted heterocyclic and aromatic groups. Many reactive dyes that are connected by azo groups are considered as azo compounds [4]. A few reactive dyes are poisonous to some creatures as well as they directly eliminated from aquatic life [5]. Furthermore, reactive dyes have water soluble nature. As a result, numerous biological and

* Corresponding authors.

physico-chemical processes can be applied for their discharge from sewage [6,7].

The treatment of dye-contaminated effluents has been accomplished using a variety of techniques, such as biological treatment [8], adsorption [9], coagulation/flocculation [10], oxidation [11], ozone treatment [12], ultrafiltration [13], photocatalysis [14] and ion-exchange [15]. Adsorption is a dependable alternative to these techniques because it is highly effective, simple to use, and has access to a variety of adsorbents.

There have been discussed numerous commonly used adsorbents that effectively remove dyes [16,17]. Although commercial activated carbon (AC) effectively remove the color but its widespread use has been constrained by its high price. For actual application of the adsorption, finding affordable and efficient adsorbents for wastewater treatment should therefore be of significant importance [18]. Researchers have demonstrated the application of various substances as adsorbents for instance clay material [19–21], natural clinoptilolite [22], composites [23], sesame hull [24], natural zeolite [25], polyurethane foam [3], modified bentonite [26], modified attapulgite [27], activated carbon [1], dehydrated beet pulp carbon [4], cross-linked succinyl chitosan [28], Gigantochloa bamboo-derived biochar [29], crop residues derived biochars [30], *Penicillium* YWO1 biomass [31], walnut husk [32], *Artocarpus odoratissimus* leaves [33], *Eucalyptus* barks [2] for eradication of organic pollutants from an aqueous solution. Agricultural by-products have demonstrated their prospective as a cheap adsorbent in this context, and they are frequently treated chemically to improve their ability to adsorb colors [34]. However, some of the adsorbents do not possess adequate adsorption capabilities against anionic dyes due to their hydrophobic/anionic nature of surfaces. Therefore, it is necessary to look for adsorbents that are more effective [35].

Pakistan is the fourth-largest producer of mangoes, with an annual production of around 17,000 m/t·y [5]. Mango leaves contains numerous glucosides like mangiferin, homomangiferin, neomangiferin and isomangiferin. These biopolymers have numerous functional moieties including hydroxyl, amino, carboxyl and phosphate etc. which provide binding sites for the molecules of dye [6]. To the best of our knowledge, no published work is available in literature on use of *Mangifera indica* (mango) leaves (MIL) powder for eosin yellow (EY) removal from an aqueous solution.

The main aim of current research is to assess the prospective of MIL powder for EY removal from wastewater at 25°C. The effect of dose of adsorbent, dye concentration, temperature and contact time on EY adsorption onto MIL powder was studied. Adsorption kinetics, thermodynamics isotherms were also investigated in detail. In addition, the regeneration of adsorbent was also investiagted.

2. Experimental set-up

2.1. Chemicals and reagents

The analytical grade chemicals were utilized in present work. Nitric acid (>99.0%, Daejung), sodium hydroxide (99.5%, Riedel-de Haen) and distilled water (DW) were used as received. The eosin yellow ($C_{20}H_8Br_4O_5$) (purity > 98%) dye was bought from Sigma-Aldrich (Massachusetts, United States). Fig. 1 represented EY's chemical structure.

2.2. Preparation of EY (adsorbate)

To prepare 1,000 ppm stock solution of EY, 1 g of EY was dissolved into 1 L of distilled water. The EY solutions of required concentration were attained by diluting the prepared stock solution with distilled water for further experiments.

2.3. Preparation of adsorbent

Fresh *Mangifera indica* leaves were gathered from nearby area of district Bahawalpur, Pakistan. To remove dust and soil impurities the washing of leaves was carried out using tap water and consequently with DW. Then, the washed leaves under direct sunlight were dried until leaves turned out brownish color. Further, they were oven dried for about 24 h at 80°C until leaves became crispy. Then, dried leaves were crushed using mechanical grinder. To remove the coloring components of leaves, the powdered leaves were dispersed into distilled water and boiled. After boiling, the leaves powder was dried for time duration of 24 h at 100°C and then sieved to attain the particle size in 75–250 μm range. Furthermore, 50 g of MIL powder was added into 1.0 M HNO_3 solution followed by vigorous stirring. Then heated the obtained mixture at 65°C for 2 h and left it the whole night at 25°C. Then, washed the contents with DW to attain pH of 7 and dried the adsorbent at 80°C until constant weight was attained. Finally, it was used for further characterization after being stored in an airtight container.

2.4. Characterization

X-ray diffraction analysis (XRD) was done through PANalytical X'Pert PRO diffractometer (Almelo, the Netherlands) for structural analysis.

2.5. Adsorption studies

Batch adsorption of EY onto MIL powder was conducted as described [5,7–12,14,36–39]. To study contact time effect, measured mass of MIL powder was shaked into 30 mg/L (25 mL) of EY solution by digital orbital shaker at 180 rpm for varying intervals of time from 10 to 90 min at temperature of 25°C. Effect of mass was evaluated by using mass range from 0.08 to 0.40 g keeping solution volume (25 mL), concentration (30 mg/L) and constant shaking speed (180 rpm) at temperature of 25°C. To demonstrate the initial

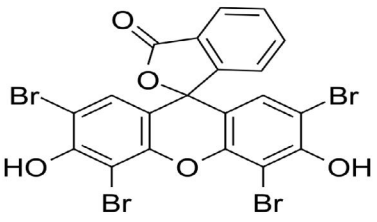

Fig. 1. Chemical structure of eosin yellow.

concentration impact, EY concentration was changed from 10 to 125 mg/L keeping MIL powder dose, contact time, shaking speed (180 rpm) and temperature constant. Temperature influence on the EY removal was evaluated by varying from 283 to 333 K by maintaining other operational parameters constant. The adsorbent was removed from solution by using filter paper after adsorption process. The absorbance of reaction medium was recorded at 520 nm and adsorption (%) of dye was calculated.

$$\%\text{Adsorption} = \frac{C_o - C_e}{C_o} \times 100 \quad (1)$$

$$q_t = \frac{C_o - C_t}{W} \times V \quad (2)$$

where C_o represents initial concentration and C_e the equilibrium concentrations of EY. Similarly, V and W are volume of EY aqueous solution and weight of adsorbent, respectively.

To check the reliability and reusability of adsorbents, desorption study was also performed by immersing a specified amount of EY loaded MIL powder into HNO_3 aqueous solution (0.1 mol/L, desorbing medium) for particular interval of time.

3. Results and discussion

3.1. XRD analysis

The chemical composition of the biomass and crystalline phases in MIL powder were investigated through X-ray diffraction analysis. Attained results are exhibited in Fig. 2. The XRD spectrum of MIL powder indicates intense diffraction peaks at 15.21°, 23.83°, 30.31°, 37.07° and 39.08° corresponding to (100), (002), (111), (220) and (101) planes, respectively [16]. The sharpness of peaks indicates high purity and crystallinity of sample. These crystalline phases reveal that a cellulose material with regular lattice properties is present. In this material, the strong secondary forces were used to bond the hydroxyl groups [6,16].

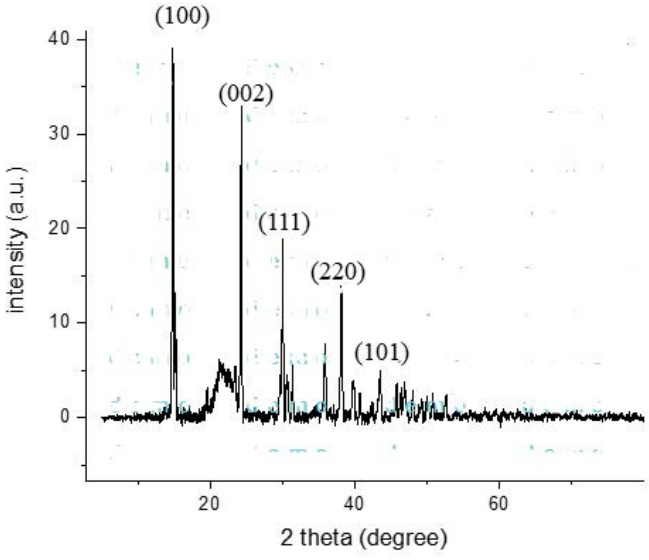

Fig. 2. X-ray diffraction pattern of MIL powder.

3.2. Effect of operating factors

3.2.1. Effect of contact time

Fig. 3a depicts contact time impact on percentage adsorption of EY from wastewater using MIL powder as adsorbent. Herein, the initial concentration of EY in solution was 30 mg/L and mass of MIL powder 0.30 g at room temperature. Results indicated that EY removal was increased from 46.02% to 84.53% with enhancement of contact time at 25°C. It can be noticed that EY removal was 93% after 75 min which was noticed as maximum removal. After it, there was no significant increase in EY discharge from wastewater. Initially, EY removal was quick because there were many empty sites onto adsorbents surface [15,17,40]. Later, it became almost constant because the pollutants molecules occupied the active sites on adsorbent surface with passing time. There was insignificant EY adsorption noticed after achieving the equilibrium at 75 min. In further experiments of EY adsorption onto MIL powder, the optimum time of 75 min was used to conduct experimental data.

3.2.2. Effect of MIL powder amount

Fig. 3b illustrates the impact of adsorbent (MIL powder) amount on the discharge of EY from wastewater at 25°C. Results demonstrated that EY (%) discharge from an aqueous solution was increased 45.14% to 93% with enhancement in MIL powder mass from 0.08 to 0.4 g. The maximum removal was attained at 0.3 g which was used as optimum mass to conduct further experiments. With further increase in adsorbent dosage it started decreasing. This was because of enhancing the number of actives sites with adsorbent dose which results in increase EY removal efficiency [11,18,41]. Contrary, the reduction in adsorption efficiency with enhancing adsorbent doses was because of aggregation of particles which result in decreasing adsorbent's surface area and number of active sites [12,30,42]. So, it was seen that dye was highly removed at 0.3 g of adsorbent dose.

3.2.3. Effect of pollutant concentration

The concentration's influence on EY discharge from wastewater was illustrated by varying from 25–125 mg/L at temperature of 25°C. Fig. 3c exhibits the attained results. It can be noted that EY (%) discharge from wastewater was declined as the EY starting concentration increased. This was associated to enhancement in the concentration gradient's ability to conquer the dye's mass transfer resistance among the aquatic and solid phases with increasing initial dye amount [22,32].

3.2.4. Effect of temperature

To elucidate the temperature impact on EY (%) discharge from wastewater, EY adsorption onto MIL powder was conducted by using temperature range from 283–333 K. Fig. 3d depicts the attained results. With increasing temperature, the increase in EY removal was observed. It represented that

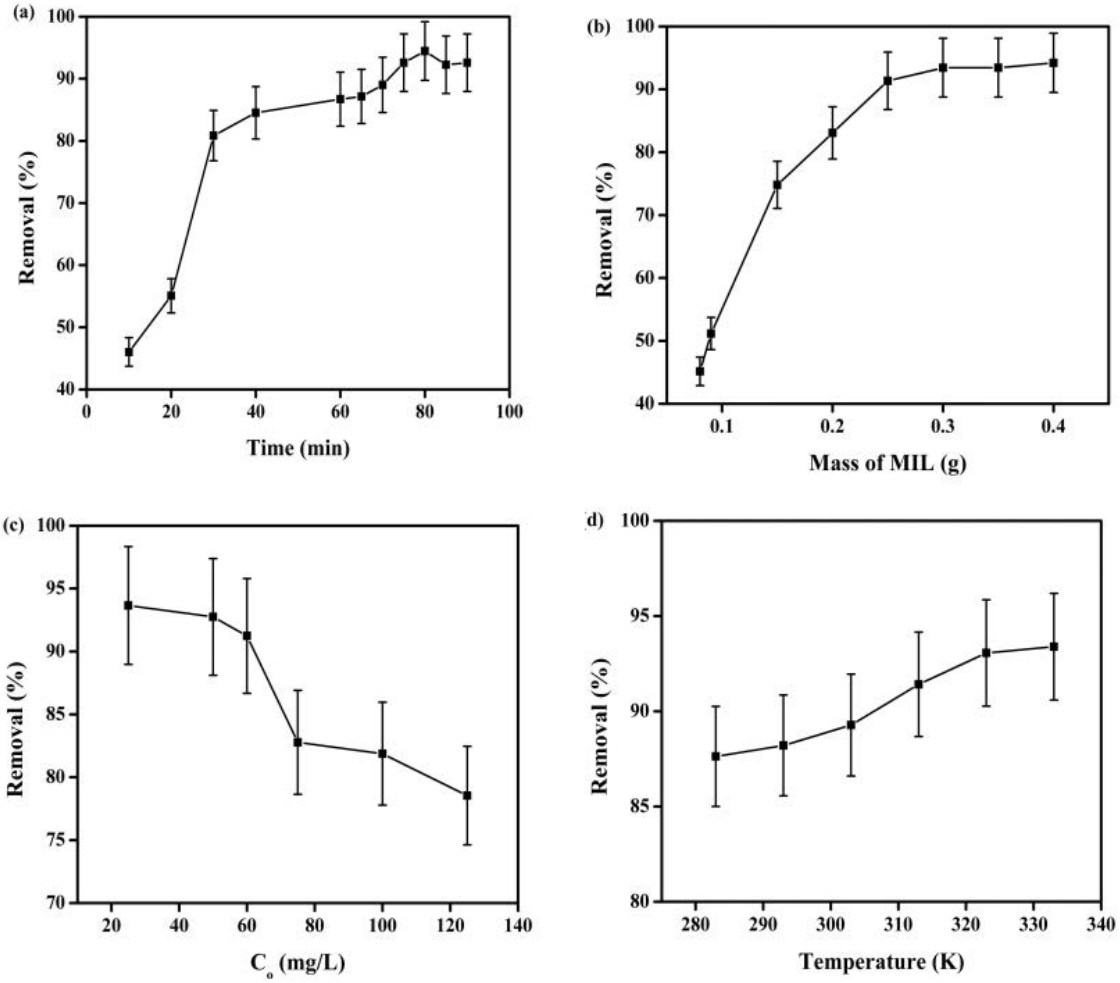

Fig. 3. (a) Effect of contact time, (b) dose of MIL powder, (c) initial eosin yellow concentration, and (d) temperature on eosin yellow release from wastewater.

EY discharge from wastewater by using MIL powder was an endothermic process. Comparison of MIL powder efficiency for EY removal from wastewater with other reported adsorbents in literature is represented in Table 1.

3.3. Adsorption isotherms

3.3.1. Two parameters non-linear adsorption isotherms

The EY adsorption onto MIL powder was illustrated through non-linear Freundlich, Langmuir, Temkin, Dubinin–Radushkevich. The software, that is, IGOR Pro WaveMetrics 6.2.1 was utilized for applying non-linear regression [17,44]. Non-linear chi-square (χ^2) analysis is a key statistical tool that is well regarded for observing which model fits best. Smaller the χ^2 value much better the model fits the data and the larger the value, the more the experimental results deviate from the model [17,32].

Chi-square test 'χ^{2}' was used to evaluate which model provided the equations with best fit.

$$\chi^2 = \sum \frac{\left(Q_e - Q_{e,m}\right)^2}{Q_{e,m}} \tag{3}$$

where $Q_{e,m}$ (mg/g) represents equilibrium capacity computed through model and Q_e (mg/g) represents equilibrium capacity determined utilizing experimental data.

Non-linear Langmuir adsorption isotherm is given as [32].

$$q_e = \frac{Q_m K_L C_e}{1 + K_L C_e} \tag{4}$$

where Q_m (mol/g) and K_L (L/mol) indicate Langmuir monolayer adsorption capability and Langmuir constant, respectively. For EY adsorption, non-linear Langmuir isotherm is represented in Fig. 4 and Table 2 is showing the measured Q_m and K_L values. The very lower chi-square value (χ^2 = 1.430) showing that the Langmuir model fits the EY adsorption onto MIL powder.

Non-linear Freundlich isotherm is denoted as [17,32]

$$q_e = K_f C_e^{1/n} \tag{5}$$

where n and K_f are the Freundlich's isotherm parameters. Freundlich isotherm plot is indicated in Fig. 4. Lower

Table 1
Comparison of adsorption capacity of MIL powder with various adsorbents reported in literature

Adsorbent	Adsorption capacity (mg/g)	References
Pineapple peels	11.76	[24]
Peanut shell	0.351	[23]
Teak leaf litter powder	31.64	[25]
Lemon peel	8.240	[31]
Date palm fronds	217	[43]
Sunflower husk	19.103	[26]
Rice husk	25.04	[21]
Oil bean seed shells based activated carbons	30.2	[28]
Wood saw dust	1.206	[19]
Clay/carbon composite	4.04	[20]
Mangifera indica leaves	39.67	Present study

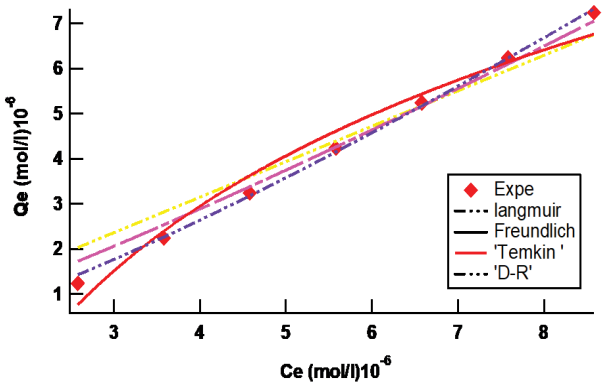

Fig. 4. Non-linear graph of Temkin, Langmuir, Dubinin–Radushkevich and Freundlich for adsorption of eosin yellow onto MIL powder from wastewater.

chi-square value (χ^2 = 4.011) depicted that EY adsorption followed Freundlich isotherm. Table 2 is depicting the experimentally measured values of Freundlich endowments (n and K_f).

Temkin adsorption isotherm is represented as:

$$q_e = \frac{RT}{b_T}\ln\left(a_T C_e\right) \tag{6}$$

where T (K) and R (J/mol·K) represent absolute temperature and gas constant, respectively and b_T and a_T are associated with heat of adsorption and equilibrium binding constant corresponding to highest binding energy, respectively. Fig. 4 depicts non-linear Temkin adsorption isotherm plot and calculated values of b_T and a_T are provided in Table 2. For it, the Chi-square result showing that Temkin adsorption isotherm was followed by EY adsorption onto MIL powder.

To differentiate EY adsorption onto mango leaves either physical or chemical adsorption, Dubinin–Radushkevich isotherm was employed [27]. Non-linear Dubinin–Radushkevich isotherm is shown as:

Table 2
Determined adsorption isotherm parameters for eosin yellow adsorption onto MIL powder

Adsorption isotherms	Determined parameters	
Langmuir isotherm	Q_m	39.67
	K_L	0.019
	χ^2	1.430
Freundlich isotherm	n	0.853
	K_f	6.089
	χ^2	4.011
Temkin isotherm	b_T	4.904
	a_T	4.509
	χ^2	8.202
Dubinin–Radushkevich isotherm	C_m	0.013
	β	0.009
	χ^2	5.811
	E	7.46

Q_m: mg/g; K_L: L/mol; K_f: mol/g; b_T: kJ/mol; A_T: L/mg; β: mol²/J²; C_m: mg/g; E: kJ/mol

$$q_e = C_m \exp\left(-\beta\varepsilon^2\right) \tag{7}$$

The Polanyi potential "ε" is shown in Eq. (8):

$$\varepsilon = RT\ln\left(1+\frac{1}{C_e}\right) \tag{8}$$

where R (J/mol·K) and T (K) reveal gas constant and absolute temperature, respectively. β indicates mean adsorption energy in Eq. (7):

$$E = \frac{1}{\sqrt{2\beta}} \tag{9}$$

Fig. 4 is representing the Dubinin–Radushkevich isotherm plot. Herein, (<8 kJ/mol) mean adsorption energy suggest the physiosorption while (>8 kJ/mol) reveal chemisorption ion-exchange processes [45]. Determined mean adsorption energy values of 7.46 kJ/mol exhibited physical adsorption of EY onto MIL powder [12,14,15,42].

3.3.2. Three parameters non-linear adsorption isotherms

The plots of 3-parameter isotherms containing Toth, Hill, Redlich–Peterson, and Sips isotherms for adsorption of eosin yellow are represented in Fig. 5.

Non-linear Redlich–Peterson isotherm is given as:

$$Q_e = \frac{K_R C_e}{1+a_R C_e^g} \tag{10}$$

where K_R, a_R and g are the Redlich–Peterson's isotherm parameters. C_e indicates liquid phase adsorbent

concentration at equilibrium and Q_e represents adsorbate loading on MIL powder adsorbent at equilibrium. Non-linear Redlich–Peterson isotherm plot is indicated in Fig. 5. Lower chi-square value (χ^2 = 6.433) depicted that EY adsorption followed Redlich–Peterson isotherm. Experimentally determined values of Redlich–Peterson constants are represented in Table 3.

Non-linear Hill isotherm is given as:

$$q_e = \frac{q_h \times C_e^{n_h}}{K_d + C_e^{n_h}} \tag{11}$$

where K_d, Q_h and n_h are Hill isotherm constants. Fig. 5 depicts the non-linear Hill isotherm plot and Table 3 is providing calculated values of K_d, n_h, and Q_h. According to the results Hill isotherm model is very good with χ^2 = 9.137 for EY adsorption onto MIL powder.

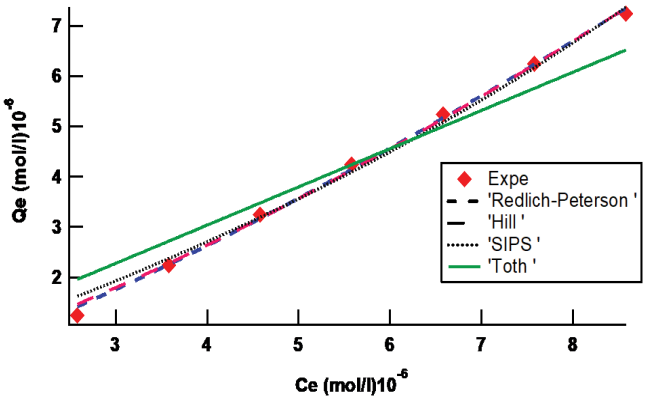

Fig. 5. Non-linear plots of Hill, Redlich–Peterson, Sips and Toth for the adsorption of eosin yellow onto mango leaves from wastewater.

Table 3
Determined endowments of three parameters non-linear adsorption isotherms for eosin yellow adsorption onto MIL powder

Adsorption isotherms	Determined parameters	
Redlich–Peterson	K_R	1.668
	a_R	8.818
	g	1.107
	χ^2	6.433
Hill isotherm	Q_h	5.158
	n_h	1.341
	K_d	0.112
	χ^2	9.137
Sips isotherm	K_s	1.013
	β_s	1.043
	a_s	5.684
	χ^2	2.367
Toth isotherm	k_T	0.956
	a_t	1.077
	T	0.381
	χ^2	1.431

Non-linear Sips isotherm is given as:

$$Q_e = K_S \frac{C_e^{\beta_s}}{1} + a_S C_e^{\beta_s} \tag{12}$$

where K_s and a_s represent Sips isotherm model constants whereas β_s indicates Sips isotherm exponent. Fig. 5 depicts the non-linear Sips isotherm plot and Table 3 is showing calculated values of K_s, β_s and a_s. The investigation showed that the value of χ^2 is 0.956. Therefore, the adsorption of EY onto MIL powder is best described by Sips isotherm model.

Non-linear Toth isotherm is given as:

$$Q = \frac{k_T C_e}{\left(a_T + C_e\right)^{1/t}} \tag{13}$$

where k_T, T and a_T indicate Toth isotherm constants. Non-linear Toth isotherm plot is indicated in Fig. 5. Lower chi-square value (χ^2 = 1.431) depicted that EY adsorption followed Toth isotherm. Experimentally determined values of Toth constants (k_T, a_T and T) are represented in Table 3.

3.4. Adsorption kinetics

EY adsorption onto MIL powder was subjected to non-linear pseudo-first-order and pseudo-second-order models for illustrating kinetics of adsorption. By applying non-linear pseudo-first-order and pseudo-second-order models calculated kinetic endowments; utilized the software IGOR Pro 6.1.2, WaveMetrics.

Non-linear pseudo-first-order equation given as:

$$Q_t = Q_e\left(1 - e^{-kt}\right) \tag{14}$$

Non-linear pseudo-second-order equation is represented as:

$$Q_t = \frac{k_2 Q_e^2 t}{1 + k_2 Q_e t} \tag{15}$$

where Q_e (mg/g) indicates the quantity adsorbed at equilibrium, t (min) represents time, Q_t represents quantity adsorbed at "t", time, k_1 and k_2 (g/mg·min) represent pseudo-first-order and pseudo-second-order rate constants.

For EY adsorption onto MIL power, the graphical representation of non-linear pseudo-first-order and pseudo-second-order kinetics is denoted in Fig. 6 and Table 4 shows the experimentally calculated constants values and theoretical Q_e values.

Table 4 presents measured 'χ^2' values. The comparison of experimental data with model-derived data generally revealed that whether the data are identical in this instance 'χ^2' would indicate a limited number and vice versa. To calculate kinetic constants for the adsorption pseudo-second-order model is more trustworthy as confirmed by the obtained lower 'χ^2' (non-linear) values.

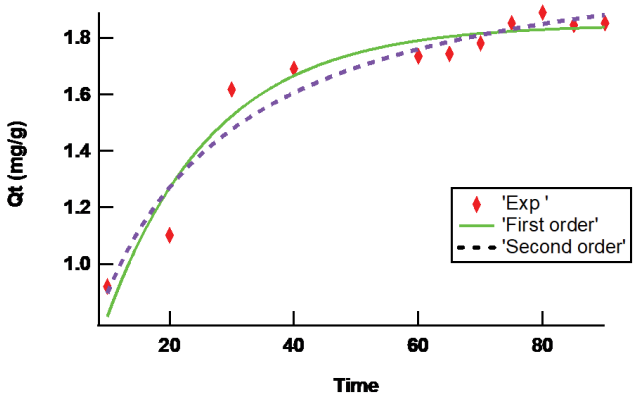

Fig. 6. Non-linear pseudo-first-order and pseudo-second-order kinetic plots regarding eosin yellow adsorption upon MIL powder from wastewater.

Table 4
Non-linear pseudo-second-order and pseudo-first-order parameters for eosin yellow adsorption onto mango leaves adsorbent

Adsorption kinetics	Calculated parameters	
Pseudo-first-order model	Q_e	1.846
	k_1	0.058
	χ^2	0.061
Pseudo-second-order model	Q_e	2.179
	k_2	0.032
	χ^2	0.063

k_1: min^{-1}; k_2: g/mg·min; Q_e: mg/g

3.5. Adsorption thermodynamics

The thermodynamics of EY adsorption onto MIL powder was investigated through determining entropy, Gibb's free energy change and enthalpy using following equations:

$$\ln K_c = \frac{\Delta S^\circ}{R} - \frac{\Delta H^\circ}{RT} \quad (16)$$

$$K_c = \frac{C_a}{C_e} \quad (17)$$

$$\Delta G^\circ = \Delta H^\circ - T\Delta S^\circ \quad (18)$$

where ΔH° (kJ/mol), R, ΔG° (kJ/mol), ΔS° (J/mol·K) and K_c denote enthalpy change, general gas constant, Gibb's free energy change, entropy change and equilibrium constant, respectively. Fig. 7 depicts the graph between $1/T$ and $\ln K_c$ for EY adsorption and calculated thermodynamic factors are presented in Table 5. The experimental outcomes revealed the endothermic nature of EY adsorption onto MIL powder as proved by the positive enthalpy change value (ΔH° = 12.13 kJ/mol) [34,35]. In addition, the positive entropy value (ΔS° = 0.058 J/mol) for EY adsorption onto

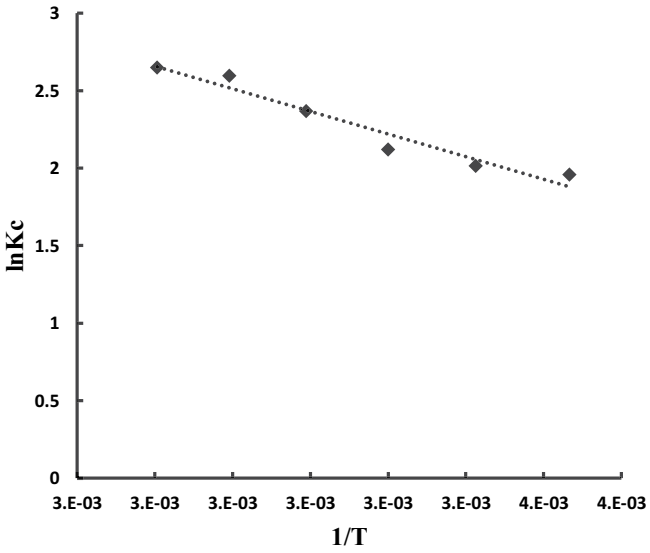

Fig. 7. $1/T$ vs. ln$k$ plot regarding eosin yellow adsorption at MIL powder.

Table 5
Thermodynamic parameters regarding eosin yellow adsorption from wastewater upon MIL powder

Temperature (K)	ΔH° (kJ/mol)	ΔS° (J/mol)	ΔG° (kJ/mol)
283	12.13	0.058	–4.42161
293			–5.00669
303			–5.59176
313			–6.17683
323			–6.76191
333			–7.34698

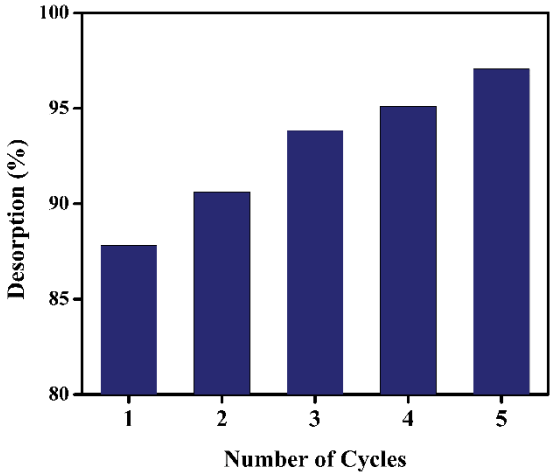

Fig. 8. Percentage desorption of eosin yellow.

MIL powder revealed that randomness increases at the adsorbent–adsorbate interface [46–48]. Negative ΔG° value exhibited that adsorption process possessed spontaneous in nature. At higher temperatures, unfeasibility of adsorption

was signified by decline in Gibb's free energy value with rising temperature [22].

3.6. Regeneration of adsorbent

In the course of treating wastewater, the MIL powder adsorbent regeneration and EY recovery are crucial criteria. There were numerous attempts made for the recovery of EY from MIL powder surface using HNO_3 (desorbing medium). In batch mode, several molarities of HNO_3 solution were utilized. For this purpose, dye loaded MIL powder (fixed amount) was soaked into nitric acid solution to recover EY. Using 1.0 mol/L of nitric acid solution, the highest recovery was attained within 10 min. Attained results for regeneration of adsorbent and recoveries of EY are represented in Fig. 8.

4. Conclusions

In current work, we illustrated EY adsorption onto MIL powder from an aqueous solution at 25°C. The EY removal was increased with increasing temperature, MIL powder mass, and contact time while decreased with initial concentration of EY. Non-linear Langmuir isotherm was well fitted to EY adsorption onto MIL powder because of the lower chi-square value (χ^2 = 1.430). The mean adsorption energy value (E = 7.46 kJ/mol) demonstrated physical nature of adsorption process of EY onto MIL powder. In addition, non-linear pseudo-second-order kinetics was obeyed by EY adsorption. Thermodynamics illustrations indicated the spontaneous and endothermic nature of EY adsorption process. Consequently, the excellent adsorption efficiency revealed that MIL powder has the potential for being an outstanding adsorbent for removing EY from aqueous solution at 25°C.

Acknowledgements

The authors are highly thankful to Government Sadiq College Women University (GSCWU), Bahawalpur for financial support.

References

[1] M. Ghaedi, H. Hossainian, M. Montazerozohori, A. Shokrollahi, F. Shojaipour, M. Soylak, M.K. Purkait, A novel acorn based adsorbent for the removal of brilliant green, Desalination, 281 (2011) 226–233.
[2] B. Balci, Basic textile dye adsorption from aqueous solution and synthetic dye bath wastewater by modified eucalyptus barks, Fresenius Environ. Bull., 25 (2016) 6124–6131.
[3] J. de Jesus da Silveira Neta, G. Costa Moreira, C.J. da Silva, C. Reis, E.L. Reis, Use of polyurethane foams for the removal of the Direct Red 80 and Reactive Blue 21 dyes in aqueous medium, Desalination, 281 (2011) 55–60.
[4] A.Y. Dursun, O. Tepe, Removal of Chemazol Reactive Red 195 from aqueous solution by dehydrated beet pulp carbon, J. Hazard. Mater., 194 (2011) 303–311.
[5] S. Shoukat, H.N. Bhatti, M. Iqbal, S. Noreen, Mango stone biocomposite preparation and application for crystal violet adsorption: a mechanistic study, Microporous Mesoporous Mater., 239 (2017) 180–189.
[6] A. Jabeen, H.N. Bhatti, S. Noreen, A. Gaffar, Adsorptive removal of 2,4,6-trichloro-phenol from wastewater by mango seed shell and its magnetic composites: batch and column study, Int. J. Environ. Anal. Chem., (2021) 1–21, doi: 10.1080/03067319.2021.1941916.
[7] M.I. Khan, S. Zafar, M.A. Khan, F. Mumtaz, P. Prapamonthon, A.R. Buzdar, *Bougainvillea glabra* leaves for adsorption of congo red from wastewater, Fresenius Environ. Bull., 27 (2018) 1456–1465.
[8] M.I. Khan, S. Zafar, A.R. Buzdar, M.F. Azhar, W. Hassan, A. Aziz, Use of *Citrus sinensis* leaves as a bioadsorbent for removal of congo red dye from aqueous solution, Fresenius Environ. Bull., 27 (2018) 4679–4688.
[9] M.I. Khan, S. Zafar, M.F. Azhar, A.R. Buzdar, W. Hassan, A. Aziz, M. Khraisheh, Leaves powder of syzgium cumini as an adsorbent for removal of congo red dye from aqueous solution, Fresenius Environ. Bull., 27 (2018) 3342–3350.
[10] M.I. Khan, S. Zafar, H.B. Ahmad, M. Hussain, Z. Shafiq, Use of morus albal leaves as bioadsorbent for the removal of congo red dye, Fresenius Environ. Bull., 24 (2015) 2251–2258.
[11] M.I. Khan, A. Shanableh, J. Fernandez, M.H. Lashari, S. Shahida, S. Manzoor, S. Zafar, A. ur Rehman, N. Elboughdiri, Synthesis of DMEA-grafted anion exchange membrane for adsorptive discharge of methyl orange from wastewaters, Membranes, 11 (2021) 166, doi: 10.3390/membranes11030166.
[12] M.I. Khan, A. Shanableh, N. Elboughdiri, M.H. Lashari, S. Manzoor, S. Shahida, N. Farooq, Y. Bouazzi, S. Rejeb, Z. Elleuch, K. Kriaa, A. ur Rehman, Adsorption of methyl orange from an aqueous solution onto a BPPO-based anion exchange membrane, ACS Omega, 7 (2022) 26788–26799.
[13] I.W. Almanassra, M.I. Khan, M.A. Atieh, A. Shanableh, Adsorption of lead ions from aqueous solution onto NaOH-modified rice husk, Desal. Water Treat., 262 (2022) 152–167.
[14] I.W. Almanassra, M.I. Khan, A. Chatla, M.A. Atieh, A. Shanableh, Utilization of palm leaves as an extraordinary adsorbent for the removal of Pb(II) from an aqueous solution, Desal. Water Treat., 271 (2022) 206–219.
[15] M.I. Khana, A. Shanableh, S. Manzoor, A. Rehman, S. Shahida, F. Ahmad, Application of United Arab Emirates *Arecaceae* leaves biochar for adsorptive removal of Rhodamine B from an aqueous solution, Desal. Water Treat., 283 (2023) 247–258.
[16] M.M.R. Khan, B. Sahoo, A.K. Mukherjee, A. Naskar, Biosorption of Acid yellow-99 using mango (*Mangifera indica*) leaf powder, an economic agricultural waste, SN Appl. Sci., 1 (2019) 1493, doi: 10.1007/s42452-019-1537-6.
[17] M.I. Khan, A. Shanableh, A.M. Alfantazi, M.H. Lashari, S. Manzoor, R. Anwer, N. Farooq, F.A. Harraz, M. Alsaiari, M. Faisal, Application of QPPO/PVA based commercial anion exchange membrane as an outstanding adsorbent for the removal of Eosin-B dye from wastewaters, Chemosphere, 321 (2023) 138006, doi: 10.1016/j.chemosphere.2023.138006.
[18] M.I. Khan, A. Shanableh, Adsorption of Rhodamine B from an aqueous solution onto NaOH-treated rice husk, Desal. Water Treat., 252 (2022) 104–115.
[19] A.O. Odiongenyi, Influence of sol–gel conversion on the adsorption capacity of crab shell for the removal of crystal violet from aqueous solution, Commun. Phys. Sci., 8 (2022) 121–127.
[20] Y. Liu, Y. Chen, Y. Shi, D. Wan, J. Chen, S. Xiao, Adsorption of toxic dye Eosin Y from aqueous solution by clay/carbon composite derived from spent bleaching earth, Water Environ. Res., 93 (2021) 159–169.
[21] M.A. Asala Faleh Ashur, Removal of Eosin stain from aqueous solution by rice husk, Plant Arch., 20 (2020) 710–716.
[22] S. Arif, S. Zafar, M. Imran Khan, S. Manzoor, A. Shanableh, J. Fernandez Garcia, M. Hayat, Removal of chromium(VI) by commercial anion exchange membrane BII from an aqueous solution: adsorption kinetic, equilibrium and thermodynamic studies, Inorg. Chem. Commun., 152 (2023) 110696, doi: 10.1016/j.inoche.2023.110696.
[23] P.P. Parichat Srisamai, P. Sudtikoonaseth, N. Kangwanrangsan, S. Iamtham, W. Jiraungkoorsku, Efficacy of Eosin dye removal by peanut shell agrowaste adsorbent, Braz. Arch. Biol. Technol., 64 (2021) 1–11.

[24] P.O.A. Fabian Audu Ugbe, V. Abiola Ikudayisi, Biosorption of an anionic dye, eosin yellow onto pineapple peels: isotherm and thermodynamic study, Int. Ann. Sci., 4 (2018) 14–19.
[25] E.O. Oyelude, J.A.M. Awudza, S.K. Twumasi, Equilibrium, kinetic and thermodynamic study of removal of eosin yellow from aqueous solution using teak leaf litter powder, Sci. Rep., 7 (2017) 12198, doi: 10.1038/s41598-017-12424-1.
[26] A.F. Hasan, M.N. Abbas, S.A. Ibrahim, Removal of eosin stain from aqueous solution by sunflower husk, J. Eng. Sustain. Dev., (2020) 1–10.
[27] S. Chen, Q. Yue, B. Gao, Q. Li, X. Xu, Removal of Cr(VI) from aqueous solution using modified corn stalks: characteristic, equilibrium, kinetic and thermodynamic study, Chem. Eng. J., 168 (2011) 909–917.
[28] C.F. Okey-Onyesolu, C.C. Okoye, D.C. Chime, Removal of eosin yellow dye from aqueous solution using oil bean seed shells based activated carbons: equilibrium, kinetics and thermodynamics studies, Int. J. Sci. Eng. Res., 9 (2018) 140–167.
[29] N. Suhaimi, M.R.R. Kooh, C.M. Lim, C.-T. Chou Chao, Y.-F. Chou Chau, A.H. Mahadi, H.-P. Chiang, N.H. Haji Hassan, R. Thotagamuge, The use of *Gigantochloa* bamboo-derived biochar for the removal of methylene blue from aqueous solution, Adsorpt. Sci. Technol., 2022 (2022) 8245797, doi: 10.1155/2022/8245797.
[30] S. Zafar, M.I. Khan, N. Elboughdiri, M.H. Lashari, A. Shanableh, S. Shahida, S. Manzoor, Adsorption performance of rice husk towards copper ions from wastewater, Desal. Water Treat., 258 (2022) 133–142.
[31] A. Bukhari, I. Ijaz, H. Zain, E. Gilani, A. Nazir, A. Bukhari, S. Raza, J. Ansari, S. Hussain, S.S. Alarfaji, R. Saeed, Y. Naseer, R. Aftab, S. Iram, Removal of Eosin dye from simulated media onto lemon peel-based low cost biosorbent, Arabian J. Chem., 15 (2022) 103873, doi: 10.1016/j.arabjc.2022.103873.
[32] M.I. Khan, M.H. Lashari, M. Khraisheh, S. Shahida, S. Zafar, P. Prapamonthon, A. ur Rehman, S. Anjum, N. Akhtar, F. Hanif, Adsorption kinetic, equilibrium and thermodynamic studies of Eosin-B onto anion exchange membrane, Desal. Water Treat., 155 (2019) 84–93.
[33] N.A.H. Mohamad Zaidi, F.N. Sallehuddin, L.B.L. Lim, M.R.R. Kooh, Surface modification of *Artocarpus odoratissimus* leaves using NaOH, SDS and EDTA to enhance adsorption of toxic crystal violet dye, Int. J. Environ. Anal. Chem., 103 (2023) 1836–1854.
[34] S. Zafar, M.I. Khan, M. Khraisheh, M.H. Lashari, S. Shahida, M.F. Azhar, P. Prapamonthon, M.L. Mirza, N. Khalid, Kinetic, equilibrium and thermodynamic studies for adsorption of nickel ions onto husk of *Oryza sativa*, Desal. Water Treat., 167 (2019) 277–290.
[35] S. Zafar, M.I. Khan, M.H. Lashari, M. Khraisheh, F. Almomani, M.L. Mirza, N. Khalid, Removal of copper ions from aqueous solution using NaOH-treated rice husk, Emergent Mater., 3 (2020) 857–870.
[36] I.W. Almanassra, M.I. Khan, M.Ali Atieh, A. Shanableh, Adsorption of lead ions from an aqueous solution onto NaOH-modified rice husk, Desal. Water Treat., 262 (2022) 152–167.
[37] M.I. Khan, T.M. Ansari, S. Zafar, A.R. Buzdar, M.A. Khan, F. Mumtaz, P. Prapamonthon, M. Akhtar, Acid green-25 removal from wastewater by anion exchange membrane: adsorption kinetic and thermodynamic studies, Membr. Water Treat., 9 (2018) 79–85.
[38] M.I. Khan, W. Liang, A.N. Mondal, Z. Yao, L. Ge, T. Xu, Adsorption of methyl orange from aqueous solution on anion exchange membranes: adsorption kinetics and equilibrium, Membr. Water Treat., 7 (2016) 23–38.
[39] M.I. Khan, S. Akhtar, S. Zafar, A. Shaheen, R. Luque, A. Rehman, Removal of Congo red from aqueous solution by anion exchange membrane (EBTAC): adsorption kinetics and themodynamics, Materials, 8 (2015) 4147–4161.
[40] M.I. Khan, J. Su, L. Guo, Development of high performance anion exchange membranes for diffusion dialysis process, Desal. Water Treat., 221 (2021) 281–290.
[41] M.A. Khan, M.I. Khan, S. Zafar, Removal of different anionic dyes from aqueous solution by anion exchange membrane, Membr. Water Treat., 8 (2017) 259–277.
[42] M.I. Khan, A. Shanableh, N. Elboughdiri, S. Manzoor, S. Mubeen, A. Rehman, Application of NaOH modified rice husk as a potential sorbent for removal of Congo red from an aqueous solution, Desal. Water Treat., 273 (2022) 221–235.
[43] N.M. Jabbar, S.D. Salman, I.M. Rashid, Y.S. Mahdi, Removal of an anionic Eosin dye from aqueous solution using modified activated carbon prepared from date palm fronds, Chem. Data Collect., 42 (2022) 100965, doi: 10.1016/j.cdc.2022.100965.
[44] S. Zafar, N. Khalid, M. Daud, M.L. Mirza, Kinetic studies of the adsorption of thorium ions onto rice husk from aqueous media: linear and non-linear approach, The Nucleus, 52 (2015) 14–19.
[45] B. Hu, H. Luo, H. Chen, T. Dong, Adsorption of chromate and para-nitrochlorobenzene on inorganic–organic montmorillonite, Appl. Clay Sci., 51 (2011) 198–201.
[46] S. Zafar, M.I. Khan, H. Rehman, J. Fernandez-Garcia, S. Shahida, P. Prapamonthon, M. Khraisheh, A. Rehman, H.B. Ahmad, M.L. Mirza, N. Khalid, M.H. Lashari, Kinetic, equilibrium, and thermodynamic studies for adsorptive removal of cobalt ions by rice husk from aqueous solution, Desal. Water Treat., 204 (2020) 285–296.
[47] S. Zafar, M.I. Khan, W. Hassan, S. Mubeen,T. Javed, S. Shahida, S. Manzoor, A. Shanableh, A. Rehman, M.L. Mirza, N. Khalid, M.H. Lashari, Application of NaOH-treated rice husk for adsorptive discharge of cobalt ions from wastewater, Desal. Water Treat., 226 (2021) 328–338.
[48] S. Zafar, M.I. Khan, A. Shanableh, S. Ahmad, S. Manzoor, S. Shahida, P. Prapamonthon, S. Mubeen, A. Rehman, Adsorption of silver, thorium and nickel ions from aqueous solution onto rice husk, Desal. Water Treat., 236 (2021) 108–122.